*Limnol. Oceanogr.*, 49(4), 2004, 934–939


# Marine diffusive boundary layers at high latitudes

*Jason Roberts*
Tasmanian Partnership for Advanced Computing, University of Tasmania, Private Bag 37, Hobart 7001, Tasmania, Australia

*Andrew McMinn*[1]
Institute of Antarctic and Southern Ocean Studies, University of Tasmania, Private Bag 77, Hobart 7001, Tasmania, Australia

*Abstract*

The thickness of marine diffusive boundary layers (DBLs) can be calculated from the friction velocity and the water density (a function of temperature and salinity). However, DBL thickness scales differently with temperature, depending on whether free-stream or friction velocity is used. We show that there are advantages to using frictional velocity for experimental scaling. Low seawater temperatures in polar areas cause DBLs to be up to 32% thicker than in temperate or tropical areas. This will have a significant effect on biological processes such as photosynthesis and respiration.

Boundary layers are regions of fluid, adjacent to a boundary, where some property of the fluid has been influenced by the boundary, compared to areas unaffected by the boundary (fluid properties in these unaffected areas are referred to as ''free-stream'' properties). The two properties of interest to this paper are fluid velocity and chemical concentration. Typical velocity and chemical concentration profiles for a boundary layer are shown in Fig. 1. Diffusive boundary layers (DBLs) are boundary layers where chemical concentration gradients are of interest.

One fundamental property of boundary layers of significance to this paper is the friction velocity ($u^*$), which is a measure of the fluid shear at the boundary and is defined by the formula $u^* = \sqrt{\nu(du/dy)}$ and has the units of velocity.

Characterization of the physical and chemical properties of DBLs associated with microbial biofilms has become critical for quantifying metabolic processes such as photosynthesis (Glud et al. 1992; Kühl et al. 1996; McMinn et al. 2000; Trenerry et al. 2002), respiration (Glud et al. 1994, 2003), sulfide cycling (Wieland and Kühl 2000), and nitrification (Larsen et al. 1997). The method most commonly used involves measuring the concentration gradient across the DBL and the thickness of the DBL. The diffusive flux ($J$) is then estimated using the one-dimensional version of Fick's Law (Revsbech and Jørgensen 1986), i.e.,

$$J = -D\frac{dC}{dy} \tag{1}$$

where $D$ is the diffusion coefficient, and $dC/dy$ is the concentration gradient across the DBL. (Table 1 contains a list of all symbols used in this paper.) Lorenzen et al. (1995) demonstrated that the use of the one-dimensional approach is legitimate under most circumstances. Røy et al. (2002) further showed that the difference between flux calculations based on either one or three dimensions is usually $<10\%$.

Using a Blasius solution (*see*, for example, White 1974), Jørgensen and Revsbech (1985) present an analysis of the factors influencing the DBL thickness for laminar boundary layers (i.e., for boundary layers where turbulent effects are negligible). Temperature effects on boundary layer thickness and diffusion coefficients were considered, but by implication, it was assumed that the ratio of the diffusive concentration boundary layer thickness to the velocity boundary layer thickness remained constant with temperature. This assumption is not valid for turbulent boundary layers (Diessler 1955). Turbulent boundary layers are common in aquatic environments, and hence, analysis methods for diffusive processes in turbulent boundary layers are required. The results for a turbulent analysis will be shown to differ significantly compared to those of a laminar flow analysis. Furthermore, the turbulent analysis must allow for variations with temperature and for differences in the ratio of the diffusive to the velocity boundary layer thickness.

Güss (1998) has shown the effect of friction velocity on DBL thickness. Gundersen and Jørgensen (1990) indirectly demonstrated the same result when they varied free-stream velocity and kept all other parameters constant, thus, in effect, changing the friction velocity.

Our goals were to (1) predict DBL thickness from friction velocity and temperature, (2) determine the appropriate velocity scaling for modeling DBLs in laboratory experiments, and (3) demonstrate that DBLs are likely to be thicker at high latitudes than in temperate and tropical regions.

This paper is concerned with flow under sea ice, which is essentially nonporous and therefore not concerned with issues relating to Darcy flow or the Brinkman layer, which are common with benthic boundary layers. Boudreau and Jørgensen (2001) provide a detailed discussion of these aspects.

## Turbulent boundary layers

Figure 1a shows a typical velocity profile for a turbulent boundary layer under sea ice. These boundary layers can be divided into three zones: (1) the viscous sublayer, (2) the overlap zone, and (3) the outer zone. Immediately adjacent

[1] To whom correspondence should be addressed. Present address: Institute of Antarctic and Southern Ocean Studies, University of Tasmania, Private Bag 252, Hobart 7001, Tasmania, Australia.

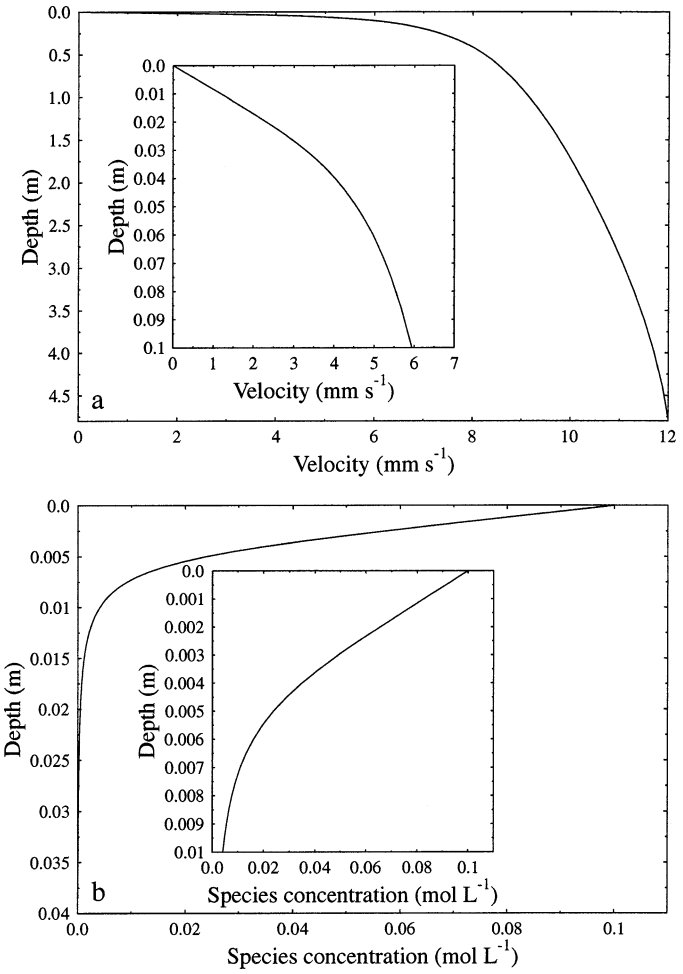


Fig. 1. (a) Turbulent velocity boundary layer profile according to White (1974) and (b) turbulent species concentration according to Martemyanov et al. (1999), both for a 5-mm diffusive boundary layer (with a free-stream velocity of 12 mm s$^{-1}$ and a temperature of −1.88°C). Depth (m) refers to height above the substrate. Note the different vertical scales. Inserts show details near the origin.

Table 1

| | |
|---|---|
| $C$ | Chemical concentration |
| $C_f$ | $\frac{\tau_\omega}{1/2\rho u^2}$ Skin fricition coefficient |
| $D$ | Molecular diffusion coefficient |
| $D_i$ | Turbulent diffusion coefficient |
| $J$ | Diffusive flux |
| $N$ | Empirical constant |
| $\mathrm{Re}_x$ | $\frac{xu_\infty}{\nu}$ Reynolds number |
| $\mathrm{Re}_x^*$ | $\frac{\delta_d u^*}{\nu}$ Reynolds number |
| $Sc$ | $\frac{\nu}{D}$ Schmidt number |
| $T$ | Temperature |
| $k$ | Empirical constant |
| $k_{yy}$ | Empirical constant |
| $u^+$ | $\frac{u}{u^*}$ Dimensionless velocity |
| $u$ | Velocity |
| $u^*$ | $\sqrt{\frac{\tau}{\rho}}$ Friction velocity |
| $u_\infty$ | Free-stream velocity |
| $x$ | Streamwise distance since inception of turbulent boundary layer |
| $y$ | Coordinate normal to the wall |
| $y^+$ | $\frac{yu^*}{\nu}$ Dimensionless normal distance from wall |
| $y_\tau$ | $\frac{\nu}{u^*}$ Dynamic length |
| Greek characters | |
| $\delta_d$ | Diffusive boundary layer thickness |
| $\mu$ | Dynamic viscosity |
| $\nu$ | Kinematic viscosity |
| $\rho$ | Density |
| $\tau$ | $\mu\frac{d\nu}{dy}$ Shear stress |
| $\tau_w$ | $\mu\frac{d\nu}{dy}\Big\|_{y=0}$ Wall shear stress |

to the surface, molecular viscous forces dominate (the zone known as the viscous sublayer), and the mean velocity varies linearly with the normal distance from the wall. In the example shown (Fig. 1), this region extends over an approximate depth of 0–25 mm. The outer zone occurs where turbulent processes dominate. On timescales significantly longer than typical eddy timescales, these turbulent processes can be represented by an additional viscosity, often called eddy or turbulent viscosity, which is typically much greater than the molecular viscosity. In the example presented (Fig. 1), this zone occurs at depths greater than approximately 1.4 m. There is also an overlap zone between the viscous sublayer and the outer zone, where both molecular and turbulent processes are important. The position and thickness of this overlap region are dependent on the relative magnitude of the molecular and turbulent viscous processes. For cases in which the turbulent viscous processes are large compared to the molecular processes, the overlap region will be both thinner and closer to the viscous sublayer than when the turbulent viscous processes are small compared to the molecular processes (White 1974).

Turbulent diffusive concentration boundary layers (*see Fig. 1b*) follow a pattern similar to that of turbulent velocity boundary layers, with one notable exception, the thickness of the various regions. The turbulent processes can be represented by an eddy or a turbulent viscosity and are the same for both velocity and chemical species concentration cases. However, the typical molecular diffusion (viscosity can be considered a diffusion of momentum) is much smaller for chemical concentration than for viscosity, i.e., the Schmidt number (the ratio of viscosity to diffusion, Sc = $\nu/D$) is much greater than unity for gaseous solutes in water. For momentum, molecular viscosity processes dominate turbulent viscosity processes near the interface (to a depth of around 25 mm; Fig. 1a). With concentration gradients, the point between where molecular processes and turbulent pro-

cesses dominate occurs closer to the interface (at a depth of around 2.5 mm; Fig. 1a), i.e., an order of magnitude thinner. The dimensionless height of this point above the interface decreases further with an increasing Schmidt number. This observation is in agreement with the findings of Diessler (1955).

Because of the variation in both viscosity and diffusion coefficients with temperature, the Schmidt number for oxygen dissolved in seawater increases with decreasing temperature. This results in a thinner DBL with decreasing temperature compared to the velocity boundary layer. However, the velocity boundary layer thickness increases with decreasing temperature, so the DBL thickness may actually be thicker at lower temperatures but be a smaller fraction of the velocity boundary layer thickness. In effect, while the dimensionless height has decreased, the denominator in the nondimensionalization (kinematic viscosity) has increased. The net result is that the physical height has actually increased.

The relatively large magnitude of the turbulent diffusion coefficient compared to the molecular diffusion coefficient and molecular viscosity results in a DBL structure that is largely similar to the velocity boundary layer but greatly attenuated in thickness. Furthermore, this attenuation is more pronounced with decreasing temperature.

## Temperature effects on viscosity and diffusion

From the above discussion, it is apparent that both the fluid viscosity and binary diffusion coefficient are important factors in estimating velocity and chemical boundary layer thicknesses. Consider the influence on viscosity and the diffusion coefficient of oxygen in seawater of temperatures between −1.88°C (the freezing temperature of seawater in the Southern Ocean) and 20°C: the kinematic viscosity ($\nu$) decreases from $1.931 \times 10^{-6}$ m$^2$ s$^{-1}$ to $1.059 \times 10^{-6}$ m$^2$ s$^{-1}$ over this temperature range (Lide 1999). Over this range, the data of Lide (1999) can be approximated by $\nu = 1.828 \times 10^{-6} - 5.319 \times 10^{-8}t + 7.011 \times 10^{-10}t^2$, where $t$ is the temperature in Celsius. The corresponding change in the molecular diffusion coefficient can be calculated using the Stokes–Einstein equation (*see*, for example, Cussler 1984), i.e.,

$$D = \frac{k_B T}{4\pi\mu R_0} \tag{2}$$

where $k_B$ (Boltzmann's constant) and $R_0$ (solute radius at the normal boiling point) are constant for the example under consideration, while the temperature $T$ and dynamic viscosity $\mu$ can vary. Therefore, Eq. 2 reduces to

$$\frac{D_{T_1}}{D_{T_2}} = \frac{T_1\mu_2}{T_2\mu_1} \tag{3}$$

between the conditions of $T_1$, $\mu_1$ and $T_2$, $\mu_2$. Using the data from Broecker and Peng (1974) for the diffusion of oxygen in freshwater at 0°C and 20°C (i.e., $D_{0°C} = 1.17 \times 10^{-9}$ m$^2$ s$^{-1}$ and $D_{20°C} = 2.06 \times 10^{-9}$ m$^2$ s$^{-1}$) and correcting for temperature and viscosity (i.e., assuming the only effect of the dissolved ions in seawater on the molecular diffusion is to change the solvent viscosity), Eq. 3 yields $D_{-1.88°C} = 1.13 \times 10^{-9}$ m$^2$ s$^{-1}$ and $D_{20°C} = 2.23 \times 10^{-9}$ m$^2$ s$^{-1}$.

## Diffusion boundary layer thickness at constant friction velocity

Using the relation from Martemyanov et al. (1999) for the turbulent diffusion coefficient $D_t(y)$

$$D_t(y) = k_{yy}\left(\frac{y}{y_\tau}\right)^N \tag{4}$$

($k_{yy}$ and $N$ are empirical constants, $y$ is the normal distance to the wall, and $y_\tau$ is a dynamic length) and the definition for the DBL thickness as being the point ($y$) where eddy diffusion is equal to molecular diffusion (Epping and Helder 1997) (i.e., $D_t = D$ at $y = \delta_d$) leads to

$$D = k_{yy}\left(\frac{\delta_d}{y_\tau}\right)^N \tag{5}$$

($\delta_d$ is the DBL thickness). Using Eq. 5, the relationships $k_{yy} = k\nu$ and $y_\tau = \nu/\sqrt{\tau/\rho}$ from Martemyanov et al. (1999), and the definition of friction velocity $u^*$ yield an equation for the DBL thickness $\delta_d$, namely

$$\delta_d = \left(\frac{D}{k}\right)^{1/N} \frac{\nu^{1-(1/N)}}{u^*} \tag{6}$$

($k$ is an empirical constant, $\nu$ is the kinematic viscosity, and $u^*$ is the friction velocity). Equation 6 can be shown to be equivalent to eqs. 3B and 4 of Boudreau (1988) (using the relation $\delta_d = D/\beta$, where $\beta$ is the mass transfer coefficient). The empirical constants $k$ and $N$ have several published values. Martemyanov et al. (1999) favor $N = 4$ and $k = 2.4 \times 10^{-4}$, while Boudreau (1988) suggests that $N = 3$ and $k = 3.02 \times 10^{-4}$ for his eq. 3B or $N = 3.378$ and $k = 2.92 \times 10^{-4}$ for his eq. 4.

Although Eq. 6 is useful, it is more helpful to write this equation explicitly in nondimensional form.

$$\mathrm{Re}^*_\delta = \frac{1}{k^{1/N}} \frac{1}{Sc^{1/N}} \tag{7}$$

($\mathrm{Re}^*_\delta$ is a Reynolds number based on the DBL thickness $\delta_d$ and friction velocity $u^*$, while Sc is the Schmidt number.) Equation 7 shows that the Reynolds number, based on the DBL thickness and friction velocity, is inversely proportional to a fractional power of the Schmidt number, with the fractional power and constant of proportionality determined from empirical data. The implications from Eq. 7 are significant for the design and analysis of experimental replication of in situ studies. The DBL thickness is a simple function of the Schmidt number (which is itself dependent on temperature), the kinematic viscosity (also dependent on temperature), and the friction velocity. Hence, to correctly scale DBL thickness, the friction velocity should be used. The friction velocity ($u^*$) can easily be determined from velocity profile measurements in the viscous sublayer region of the flow. Such a velocity profile measurement will allow the determination of the velocity gradient ($du/dy$) and hence

Table 2. Ratio of diffusive boundary layer thickness (i.e., $\delta_{d1}/\delta_{d2}$) for temperatures of −1.88°C and 20°C, for constant friction velocity.

| $N$ | $\delta_{d1}/\delta_{d2}$ | Reference for $N$ |
|---|---|---|
| 4 | 1.324 | Martemyanov et al. (1999) |
| 3 | 1.190 | Boudreau (1988) |
| 3.378 | 1.248 | Boudreau (1988) |
| Laminar | 1.493 | Jørgensen and Revsbech (1985) |

the calculation of the friction velocity using the following relationship:

$$u^* = \sqrt{\nu \frac{du}{dy}}$$

In essence, this is identical to the determination of the diffusive flux ($J$) from the concentration gradient ($dC/dy$) using Fick's Law.

Scaling with friction velocity rather than free-stream velocity also significantly simplifies the calculation of temperature effects on DBL thickness. Scaling with friction velocity requires only an application of Eq. 7 to calculate the change in boundary layer thickness. However, if free-stream velocity scaling is used, empirical-based relations for the skin friction coefficient and a knowledge of the free-stream distance from the time of turbulence inception are required in addition to Eq. 7.

*Temperature effects*—Keeping all other parameters in Eq. 7 constant (i.e., constant friction velocity) and varying the temperature will vary both the kinematic viscosity and molecular diffusion (and therefore the Schmidt number) and hence the DBL thickness. (Note that the friction velocity can be kept constant while varying the temperature, by adjusting the free-stream velocity, to alter the velocity gradient in the viscous sublayer.)

Consider the difference in DBL thickness between −1.88°C (the freezing temperature of seawater in the Southern Ocean) and 20°C. As discussed above, the kinematic viscosity decreases from $1.931 \times 10^{-6}$ m$^2$ s$^{-1}$ to $1.059 \times 10^{-6}$ m$^2$ s$^{-1}$ over this temperature range (Lide 1999), while the molecular diffusion coefficient increases from $1.13 \times 10^{-9}$ m$^2$ s$^{-1}$ to $2.23 \times 10^{-9}$ m$^2$ s$^{-1}$.

Using these values in Eq. 7 yields the results presented in Table 2; Fig. 2. The ratios of the DBL thickness at −1.88°C to 20°C have a spread of 1.190–1.324, depending on the empirical data fit selected for $k$ and $N$. The results for the laminar flow solution of Jørgensen and Revsbech (1985) are included for comparison. Calculation of the laminar flow case required direct knowledge of the streamwise distance $x$ and the free-stream velocity $u_\infty$ taken as $x = 100$ m and $u_\infty = 10$ mm s$^{-1}$ for the turbulent case and the laminar (temperature dependent) free-stream velocity calculated using the Blasius solution (*see*, for example, White 1974) to give the same friction velocity. Note that the laminar flow Reynolds numbers (based on length scale $x$) are around $1–3 \times 10^6$, well above the recommended $5 \times 10^5$ for laminar flow.

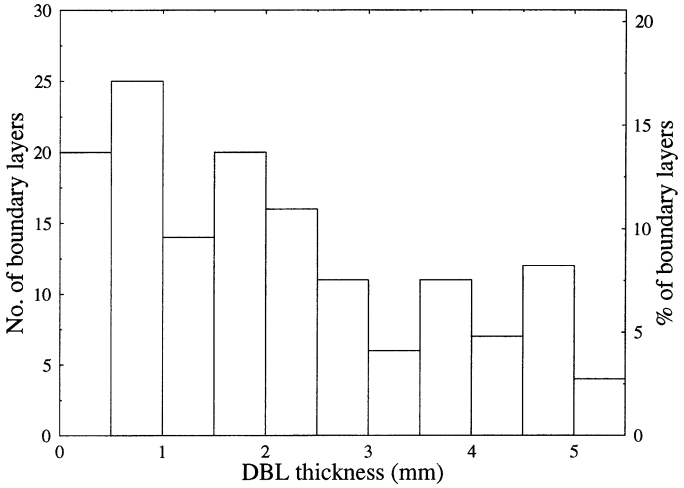


Fig. 2. Histogram showing the size distribution of DBLs from beneath sea ice. Data taken from Cape Evans (McMinn et al. 2000; Trenerry et al. 2002) and east Antarctic pack ice (McMinn unpubl. data).

## Diffusion boundary layer thickness at constant free-stream velocity

Consider the case for constant free-stream velocity rather than constant friction velocity. Below Antarctic fast ice, typical DBL thicknesses are between 0.1 and 5.0 mm. Under these conditions, the Schmidt number is >1,500; therefore, the DBL will have a maximum thickness of $y^+ < 1.5$ (Diessler 1955). Results for sand roughness elements reported in Hinze (1975) suggest that for roughness elements of a height less than $y^+ < 5$, the effect of roughness will be minimal. This corresponds to a height of roughness elements in the range 1.0–16.7 mm for the data given above. As the height of roughness elements for the seawater–ice water interface is below this value (McMinn et al. 2000), the flow can be thought of as flow over a smooth plate. For smooth, flat plates, White (1974) suggests that the skin friction coefficient $C_f$ is a function of the Reynolds number ($\mathrm{Re}_x$),

$$C_f = \frac{\tau}{1/2\rho\nu^2} = \frac{0.455}{\ln^2 0.06\mathrm{Re}_x} \tag{8}$$

where the skin friction coefficient and the friction velocity are related through the shear stress,

$$v^* = \sqrt{\tau/\rho} = \sqrt{C_f v^2/2} \tag{9}$$

Combining Eqs. 7–9 allows us to compare DBL thickness for the case of constant free-stream velocity.

$$\frac{\delta_{d1}}{\delta_{d2}} = \left(\frac{Sc_2}{Sc_1}\right)^{1/N} \frac{\nu_1}{\nu_2} \frac{\ln\ 0.06\mathrm{Re}_{x2}}{\ln\ 0.06\mathrm{Re}_{x1}} \tag{10}$$

where $\mathrm{Re}_{x1}$ can be evaluated using Eqs. 7 and 8 for a known DBL thickness, and $\mathrm{Re}_{x2} = \mathrm{Re}_{x1}(\nu_1/\nu_2)$ (i.e., direct knowledge of $x$ is never required).

*Temperature effects*—Applying Eq. 10 to the case of a 5-mm DBL at $T_1 = -1.88$°C and $u_\infty = 10$ mm s$^{-1}$ gives the results in Table 3.

Table 3. Ratio of DBL thickness (i.e., $\delta_{d1}/\delta_{d2}$) for temperatures of −1.88°C and 20°C, for $\delta_{d1}$ = 5 mm and constant free-stream velocity ($\mu_\infty$ = 10 mm s$^{-1}$).

| $k$ | $N$ | $\delta_{d1}/\delta_{d2}$ | Reference for $k$ and $N$ |
|---|---|---|---|
| $2.4\times10^{-4}$ | 4 | 1.248 | Martemyanov et al. (1999) |
| $3.02\times10^{-4}$ | 3 | 1.262 | Boudreau (1988) |
| $2.92\times10^{-4}$ | 3.378 | 1.323 | Boudreau (1988) |
| Laminar | — | 1.350 | Jørgensen and Revsbech (1985) |

These values are noticeably different from those estimated from constant friction velocity (Table 2).

The above examples show the importance of the proper selection of scaling for the experimental approximation of in situ processes. For DBL experiments, the proper velocity scaling is the wall friction velocity, not the free-stream velocity. In practice, the setting of an experimental value for the friction velocity would be an iterative process. For a given water temperature and salinity (and hence viscosity), run the experiment at a known free-stream velocity and measure the resultant velocity profile. Calculate the velocity gradient in the viscous sublayer, and calculate the friction velocity from the formula

$$u^* = \sqrt{\nu \frac{du}{dy}}$$

Adjust the free-stream velocity (and remeasure the velocity profile) until the correct friction velocity is obtained.

DBLs beneath Antarctic sea ice can be up to 5 mm thick (McMinn et al. 2000), which is unusually thick compared to previously reported values elsewhere (Fig. 2). However, if the free-stream velocity, temperature, and length scale are known, the DBL thickness can be estimated from Eq. 6, with Eqs. 8 and 9 providing the required relationship between length scale, free-stream velocity, and friction velocity. The effect on DBL thickness, keeping velocity constant, of a change in temperature from 20°C to −1.9°C is demonstrated

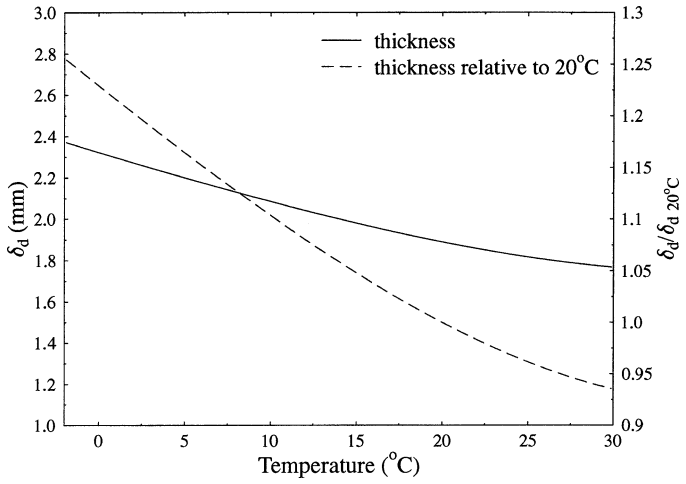


Fig. 3. Diffusive boundary layer thickness as a function of temperature and thickness relative to 20°C for $N$ = 3.378, $k$ = 2.92 × $10^{-4}$, and $u^*$ = 10 mm s$^{-1}$.

Table 4. Free-stream velocity (m s$^{-1}$) using Eqs. 3 and 7 for a temperature of −1.88°C and a length scale of $x$ = 100 m.

| $\delta_d$ (mm) | $N$=4 $k$=2.4×10$^{-4}$ | $N$=3 $k$=3.02×10$^{-4}$ | $N$=3.378 $k$=2.92×10$^{-4}$ |
|---|---|---|---|
| 5.0 | $10.5\times10^{-3}$ | $10.5\times10^{-3}$ | $10.3\times10^{-3}$ |
| 1.0 | $61.5\times10^{-3}$ | $61.4\times10^{-3}$ | $60.4\times10^{-3}$ |
| 0.1 | 0.741 | 0.739 | 0.728 |

in Fig. 3. In typical polar conditions, a 5-mm DBL would be produced by a free-stream velocity of 10.3 mm s$^{-1}$, a 1.0-mm DBL would be produced by a free-stream velocity of 60 mm s$^{-1}$, and a 0.1-mm DBL would be produced by a free-stream velocity of 728 mm s$^{-1}$ (Table 4). These measurements are consistent with observed currents and DBL thicknesses beneath sea ice. Published in situ DBL measurements are compared with results presented in this study (Table 5). The inferred friction velocities are consistent with the values presented in Wimbush and Munk (1970). The thicker-than-expected DBLs from underneath sea ice, up to 5.25 mm (Fig. 2), can be explained by the low current speeds (<2 mm s$^{-1}$). Friction velocity has been shown to be a more significant measure of velocity than free-stream velocity. However, friction velocities were not available for the studies reported in Table 5 and have been inferred using Eq. 6.

In addition to changing DBL thickness, temperature can affect microbial mats in a number of different ways. Wieland and Kühl (2000) examined the effects of a 15° temperature change on a *Cyanobacteria* mat from a tropical hypersaline lake. They reported major changes in photosynthesis and respiration with increasing temperature as a result of decreasing pH, increased heterotrophic activity, enzymatic activity and sulfide oxidation, and changed mat morphology. Similarly, Glud et al. (2003) reported temperature effects on oxygen uptake in marine sediments from Denmark. There, DBL thicknesses varied between 299 and 706 μm between summer and winter. These values were at the lower end of in situ measurements, which have mostly been taken from deep water (Glud et al. 2003). They attributed this difference

Table 5. Published in situ DBL measurements and inferred friction velocity ($u^*$) from Eq. 6.

| Reference | DBL (mm) | Inferred $u^*$ (mm s$^{-1}$) | Note |
|---|---|---|---|
| Lorke et al. (2003) | 0.16–0.84 | 2.5–13.3 | 1 |
| Glud et al. (2003) | 0.45 | 4.7 | 2 |
| Gundersen and Jørgensen (1990) | 0.48–0.68 | 3.1–4.4 | 3 |
| Archer et al. (1989) | 0.5–1.5 | 1.4–4.3 | 4 |
| Archer et al. (1989) | 3.5 | 0.61 | 5 |
| Figure 2 (herein) | 0.25–5.25 | 0.45–9.5 | 6, 7 |

Notes (1) Benthic, temperature not given, assumed to be 8°C for calculation of $u^*$; (2) Benthic, average value of DBL, at a temperature of 8°C; (3) Benthic, at a temperature of 8°C; (4) Benthic, typical values, temperature not given, assumed to be 8°C for calculation of $u^*$; (5) Benthic, maximum values from one cruise, temperature not given, assumed to be 8°C for calculation of $u^*$; (6) Sea ice, at a temperature of −1.88°C; (7) The inferred friction velocity is in good agreement with ocean-bottom estimates of 0.5–3 mm s$^{-1}$ in Wimbush and Munk (1970).

to slower current flow at greater depths, but our analysis infers that the colder water temperatures at greater depths would also make a significant contribution. It is likely that the seasonal and depth variations in DBL thickness reported in many other studies are also at least partly due to temperature effects on DBL thickness.

The above results show that temperature will affect the DBL thickness, not only in terms of absolute thickness but also the thickness relative to the velocity boundary layer thickness. Temperature effects alone account for a 19–32% thickening of the DBL beneath sea ice (depending on the value of the empirical coefficient $N$ chosen) compared to temperate/tropical DBLs. This compares with an estimate of 40% by Jørgensen (2001).

Most research on the biological effects of current velocity on DBL thickness has used free-stream velocity rather than friction velocity (Glud et al. 1992; Lorenzen et al. 1995; McMinn et al. 2000). The DBL thickness scales differently with temperature, depending on how the velocity is scaled, and care must be taken for experimental design. For example, if an experiment (conducted at the in situ temperature) is reliant on a certain DBL thickness, then the experimental velocity scaling should be to give the same friction velocity as the in situ friction velocity. A further advantage of scaling with friction velocity is that friction velocity is a fundamental scaling parameter of the DBL thickness and therefore requires no further assumptions. However, scaling with free-stream velocity requires further empirical relationships (such as Eq. 8) to relate free-stream velocity back to friction velocity.

## *References*


ARCHER, D., S. EMERSON, AND C. R. SMITH. 1989. Direct measurements of the diffuse sublayer at the deep seafloor using microelectrodes. Nature **340:** 623–626.

BOUDREAU, B. P. 1988. Mass-transport constraints on the growth of discoidal ferromanganese nodules. Am. J. Sci. **288:** 777–797.

———, AND B. B. JØRGENSEN. 2001. The benthic boundary layer: Transport processes and biochemistry. Oxford Univ. Press.

BROECKER, W. S., AND T. H. PENG. 1974. Gas exchange between air and sea. Tellus **XXVI:** 21–35.

CUSSLER, E. L. 1984. Diffusion mass transfer in fluid systems. Cambridge Univ. Press.

DIESSLER, R. G. 1955. Analysis of turbulent heat transfer, mass transfer, and friction in smooth tubes at high prandtl and schmidt numbers. Technical report TR1250, National Advisory Committee for Aeronautics.

EPPING, E. H. G., AND W. HELDER. 1997. Oxygen budgets calculated from in situ oxygen microprofiles for northern adriatic sediments. Continental Shelf Res. **17:** 1735–1764.

GLUD, R. N., J. K. GUNDERSEN, B. B. JØRGENSEN, N. P. REVSBECH, AND H. D. SCHULZ. 1994. Diffusive and total of deep-sea sediments in the eastern South Atlantic Ocean: In situ and laboratory measurements. Deep-Sea Res. **41:** 1767–1788.

———, ———, H. RØY, AND B. B. JØRGENSEN. 2003. Seasonal dynamics of benthic O2 uptake in a semienclosed bay: Importance of diffusion and faunal activity. Limnol. Oceanogr. **48:** 1265–1276.

———, N. B. RAMSING, AND N. P. REVSBECH. 1992. Photosynthesis and photosynthesis-coupled respiration in natural biofilms quantified with oxygen microsensors. J. Phycol. **28:** 51–60.

GUNDERSEN, J. K., AND B. B. JØRGENSEN. 1990. Microstructure of diffusive boundary layers and the oxygen uptake of the sea floor. Nature **345:** 604–607.

GÜSS, S. 1998. Oxygen uptake at the sediment–water interface simultaneously measured using a flux chamber method and microelectrodes: Must a diffusive boundary layer exist. Estuarine Coastal Shelf Sci. **46:** 143–156.

HINZE, J. O. 1975. Turbulence. McGraw-Hill.

JØRGENSEN, B. B. 2001. Life in the diffusive boundary layer, p. 348–373. *In* B. P. Boudreau and B. B. Jørgensen [eds.], The benthic boundary layer: Transport processes and biochemistry. Oxford Univ. Press.

———, AND N. P. REVSBECH. 1985. Diffusive boundary layers and the oxygen uptake of sediments and detritus. Limnol. Oceanogr. **30:** 111–122.

KÜHL, M., R. N. GLUD, H. PLOUG, AND N. B. RAMSING. 1996. Microenvironmental control of photosynthesis and photosynthesis-coupled respiration in an epilithic cyanobacterial biofilm. J. Phycol. **32:** 799–812.

LARSEN, L. H., T. KJAER, AND N. P. REVSBECH. 1997. A microscale $NO_3^-$ biosensor for environmental applications. Anal. Chem. **69:** 3527–3531.

LIDE, D. R. [ED.]. 1999. Handbook of chemistry and physics, 80th ed. CRC Press.

LORENZEN, J., R. N. GLUD, AND N. P. REVSBECH. 1995. Impact of microsensor-caused changes in diffusive boundary layer thickness on $O_2$ profiles and photosynthetic rates in benthic communities of microorganisms. Mar. Ecol. Prog. Ser. **119:** 237–241.

LORKE, A., B. MÜLLER, M. MAERKI, AND A. WÜEST. 2003. Breathing sediments: The control of diffusive transport across the sediment–water interface by periodic boundary-layer turbulence. Limnol. Oceanogr. **48:** 2077–2085.

MARTEMYANOV, S., E. SKURYGIN, AND J. LEGRAND. 1999. Turbulent mass transfer in the developing diffusion layer at large schmidt numbers. Int. J. Heat Mass Transfer **42:** 2357–2362.

MCMINN, A., C. ASHWORTH, AND K. RYAN. 2000. In situ net primary productivity of an antarctic fast ice bottom algal community. Aquat. Microb. Ecol. **21:** 177–185.

REVSBECH, N. P., AND B. B. JØRGENSEN. 1986. Microelectrodes: Their use in microbial ecology. Adv. Microb. Ecol. **9:** 293–352.

RØY, H., M. HUTTEL, AND B. B. JØRGENSEN. 2002. The role of small-scale sediment topography for oxygen flux across the diffusive boundary layer. Limnol. Oceanogr. **47:** 837–847.

TRENERRY, L. J., A. MCMINN, AND K. G. RYAN. 2002, In situ oxygen microelectrode measurements of bottom ice algal production in McMurdo Sound, Antarctica. Polar Biol. **25:** 72–80.

WHITE, F. M. 1974. Viscous fluid flow. McGraw-Hill.

WIELAND, A., AND M. KÜHL. 2000. Short-term temperature effects on oxygen and sulphide cycling in a hypersaline cyanobacterial mat (Solar Lake, Egypt). Mar. Ecol. Prog. Ser. **196:** 87–102.

WIMBUSH, M., AND W. MUNK. 1970. The benthic boundary layer, p. 731–758. *In* A. E. Maxwell [ed.], The sea, 4, part 1. Wiley.


*Received: 24 June 2003*
*Accepted: 18 February 2004*
*Amended: 28 March 2004*